

STATE ESTIMATION AND ENERGY MANAGEMENT OF MICROGRID ENERGY STORAGE SYSTEM USING PARTICLE FILTER AND MARKOV CHAIN MONTE CARLO

Libin Yang^{*,**} Tingxiang Liu^{*,**} Zhengxi Li^{*,**} Wanpeng Zhou^{*,**} Zhengxi Li^{*,**} and Na An^{*,**}

Abstract

Microgrid energy storage systems play a crucial role in power systems, but their state estimation and energy management face challenges due to the uncertainty and complexity of system state and energy changes. A particle filter-based method for estimating the charge state and predicting the lithium-ion batteries lifespan was proposed to address the issues of state estimation and energy management in microgrid energy storage systems. At the same time, a microgrid energy storage system energy management model was constructed by integrating Markov chain and Monte Carlo methods. The research results indicated that the SOC estimation results using the open circuit voltage definition were more accurate than those using the ampere-hour integral definition, showing an approximately linear change in voltage within the SOC range of 20%–100%. In terms of microgrid energy management, the total energy capacity of energy storage batteries and electric vehicle (EV) batteries was 8 kWh and 16 kWh, respectively. By considering the prediction of EV and optimising energy management during electricity usage time, operating costs were reduced. From the above experimental results, both proposed methods have achieved good results in state prediction and energy management of microgrid energy storage systems, providing an effective theoretical basis and empirical support for the estimation and prediction of lithium-ion batteries and energy management of microgrids.

Key Words

Particle filtering; Markov chain; microgrid; energy storage; energy management

1. Introduction

Due to the high nonlinearity, time-varying, uncertainty, and multiple constraints of microgrids, accurate estimation and effective management of system states are quite challenging. Studying efficient and reliable state estimation methods and energy management strategies for microgrid energy storage systems is not only significant for ensuring the microgrid stable operation, but also a research hotspot in the field [1]–[3]. Based on the prior art, the proposed method integrates the advantages of the Markov chain Monte Carlo (MC) technique under the framework of particle filter, innovatively reducing the computational complexity, while maintaining the high precision and robustness of system state estimation. The method effectively solves the performance bottleneck of traditional particle filters in complex dynamic microgrid energy storage systems by optimising important sampling and resampling algorithms. In addition, with the help of advanced algorithm design, this method can enhance the adaptability of nonlinear and time-varying characteristics in the state estimation of microgrid energy storage systems and provide the possibility of real-time calculation. In terms of energy management strategy, the method introduces the control theory based on a predictive model, which optimises energy storage scheduling, improves operation efficiency, and prolongs equipment life while ensuring system stability. Through these innovations, the proposed method provides a new technical approach for the efficient and reliable operation of microgrids. The Markov chain MC method is an effective statistical method widely used for state estimation of complex systems. However, its high computational complexity makes it difficult to meet the real-time operation needs of microgrid systems [4]. On the contrary, particle filter methods have shown inherent advantages in dealing with estimation problems of complex systems such as nonlinear and non-Gaussian [5], [6]. It can improve estimation accuracy and robustness through importance sampling and resampling steps. Therefore, research on state estimation of microgrid energy storage systems based on particle filtering and

* Economic and Technological Research Institute of State Grid Qinghai Electric Power Company, Xining 810000, China; e-mail: L18309717153@126.com

** Clean Energy Development Research Institute of State Grid Qinghai Electric Power Company, Xining 810000, China
Corresponding author: Tingxiang Liu

Markov chain MC methods has attracted much attention. Proper energy management can not only ensure the continuous operation of microgrids in emergencies, peak load, and other situations that require a large amount of electricity but also provide maximum power guarantee during daily operation, extend the service life of equipment, and achieve optimisation of efficiency [7]–[9]. Therefore, researching efficient and convenient energy management strategies for microgrids can significantly improve the operational efficiency and service quality of microgrids. In this context, this article aims to explore a state estimation method for microgrid energy storage systems based on particle filtering and Markov chain MC, combined with effective energy management strategies, to provide a theoretical basis and practical solutions for microgrid design and operation.

The research is divided into four parts. The first part summarises and analyses the current research status, and the second part proposes a state estimation and energy management method for microgrid energy storage systems based on particle filtering and Markov chain MC. The comprehensive management of microgrid energy storage systems is carried out from two aspects: lithium-ion (LTO) battery state of charge (SOC) estimation and energy management. The third part verifies the effectiveness of state estimation and energy management methods for microgrid energy storage systems through simulation experiments. The fourth part summarises the core research content.

2. Related Works

In recent years, research on state estimation and energy management of microgrid energy storage systems has gradually become more abundant. Meng *et al.* proposed two types of distributed estimators, one for asymptotic estimation and the other for finite time estimation. Through simulation experiments, it was verified that the proposed control method can achieve the charge and discharge balance of all battery cells to meet the total demand [10]. Khalid *et al.* discussed in detail the issues of protecting blind spots and delineating intended islands. At the same time, a 3 MW/9 MWh microgrid project at Florida International University and its experimental results were also introduced [11]. Joshi *et al.* proposed a grid frequency regulation control architecture based on voltage angle deviation at common coupling points. Compared with traditional frequency drop coating methods, this scheme achieved a performance improvement of over 20% [12]. Daneshvar *et al.* used autoregressive integral moving average and fast-forward selection methods for risk modelling and achieved intraday dynamic energy management through horizontal energy allocation. This method achieved an 8.51% increase in energy costs [13]. Islam *et al.* proposed a dual optimisation strategy that considers the scheduling of renewable energy and battery storage systems. Results indicated that microgrid operating costs using this strategy were reduced by 7% and 6% during the scheduling and allocation stages, respectively [14].

In addition, the application of particle filtering and Markov chain MC in various fields is gradually deepening. Pozna *et al.* developed a novel PF-PSO algorithm that not only randomly generated particle swarm but also precisely adjusted the search range. By reducing the cost function of the PF-PSO algorithm, the energy consumption of the fuzzy control system can be reduced [15]. Gunatilake *et al.* proposed a novel dual antenna system based on high-frequency radio frequency identification technology, combined with the Gaussian process and particle filter algorithm, for high-precision positioning of robots in pipelines. This system had millimeter-level accuracy and achieved high-precision positioning up to 50 m without significant estimation drift. The application effect of this system in actual water pipes was verified through experiments [16]. Ballesio *et al.* studied the filtering problem of partially observable diffusion and proposed a resampling method based on optimal Wasserstein coupling. Considering the mean square error (MSE) of the filter, they developed a multi-level MC (MLMC) method to improve the performance of particle filters. The effectiveness of this method was verified by testing the convergence of the algorithm in different scenarios and comparing computational costs [17]. Dalgaty *et al.* tried to apply resistance value storage technology to intelligent system learning for edge computing. They proposed a machine learning scheme that utilised memory to resist variability and implemented a Bayesian machine learning model using Markov chain MC sampling method on 16384 device arrays that were manufactured. Clinical trials showed that this method can successfully identify malignant tissues and arrhythmia and had good performance in up to 10 million durability tests [18].

Srilakshmi and Singh proposed an optimised operation strategy for community microgrids based on photovoltaics, energy storage systems, and electric vehicles (EV), utilising the bidirectional current flow strategy of EVs to provide electricity for households and the power grid. The optimisation was achieved using mixed integer linear programming, and the effectiveness of this strategy was demonstrated through comparative analysis [19]. Bakhtiari *et al.* proposed an improved Metropolis-coupled Markov chain MC 3 simulation method to predict the stochastic behaviour of different sources of uncertainty in independent renewable energy microgrid planning. The results showed that the proposed model accurately characterised the probability distribution, sample continuity, time dependence, correlation between different uncertainty sources, as well as short-term and long-term trends of uncertainty sources [20]. Salim *et al.* proposed two cascaded schemes to improve power quality, namely, total harmonic distortion (THD) minimisation and voltage regulation. The results showed that the proposed scheme ensured power factor, high efficiency, system power quality, and reliability under different load conditions by optimising parameters through a particle swarm optimisation algorithm [21]. Gadanayak and Mallick proposed an intelligent non-guided protection strategy based on iterative filtering, empirical mode decomposition, and extreme learning machine for inverter-dominated microgrids. The results indicated that

this strategy effectively detected faults and identified fault phases. It was widely validated in standard microgrid models with different topologies and operating modes for both arc and non-arc faults [22].

Existing research on microgrid state estimation faces challenges in terms of nonlinear and non-Gaussian distributions: (1) Particle filters and Markov chain MC methods have been introduced, which are more suitable for dealing with complex state estimation problems in microgrids; (2) A new strategy has been developed that combines state estimation with daily operational decision-making, improving the precision and efficiency of microgrid management; (3) A new algorithm has been implemented that can adapt to the constantly changing conditions of microgrids, such as the unstable output of renewable energy and load fluctuations. The effectiveness of these methods has been verified through simulation, and it is hoped that they can bring better operational performance and cost-effectiveness to microgrids.

3. State Estimation and Energy Management of Microgrid Energy Storage System Using Particle Filter and Markov Chain Monte Carlo

This article first introduces a particle filter-based method for estimating charge state and predicting the ITO batteries lifespan. This method uses an equivalent circuit model (ECM) to indirectly obtain the SOC of ITO batteries by constructing a nonlinear mapping relationship. In addition, the use of Markov chains to obtain the parameters stationary distribution to achieve optimal estimation has improved energy management efficiency.

3.1 Charge State Estimation and Lithium-ion Batteries Lifespan Prediction using Particle Filter

The ECM characterises ITO battery characteristics through circuit elements, such as resistors, capacitors, and voltage sources, and is critical for state estimation and lifetime prediction. The OCV voltage source describes the electromotive force of the battery without load, and its nonlinear relationship with the SOC reflects the true voltage. The resistance represents an immediate voltage drop, while the RC network exhibits charge transfer and polarisation effects. ECM simplifies the electrochemical process and makes the energy system easy to analyse and control. The first-order RC model balances simplicity with precision, as shown in Fig. 1.

In this model, the input variables include the current (I) and the open circuit voltage (OCV). The left section of the circuit, comprising resistors R_d , current-controlled current sources C_N , and capacitors, receives these inputs, simulating the self-discharge, charge state, and battery capacity characteristics. The right section includes a resistor R and a first-order RC network $R_p C_p$, simulating the transient response of the battery during a sudden change in current. To achieve SOC estimation that minimises polarisation effects, an online estimation method

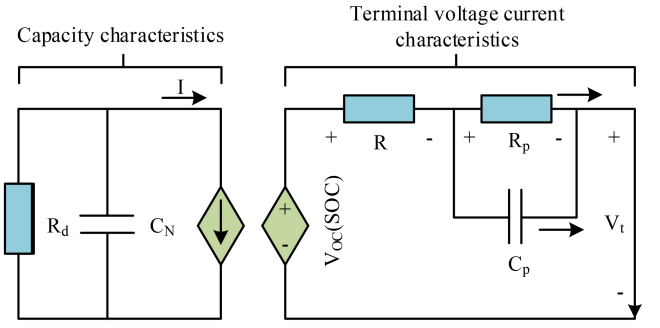


Figure 1. A first-order EC for lithium-ion batteries.

using OCV is proposed, and the SOC value is indirectly obtained through the nonlinear mapping relationship between OCV and SOC. The SOC refers to a dimensionless ratio, typically expressed as a percentage, indicating the remaining capacity of a battery relative to its full capacity. It is an essential parameter that mirrors the current state of energy in the battery, serving as a gauge for the remaining runtime and charge needed. In this investigation, the SOC is indirectly estimated through the nonlinear mapping of OCV to SOC, leveraging the constructed battery model to provide an accurate approximation. OCV is the voltage of a battery when it is not under any electrical load, meaning no current is flowing into or out of the battery. It is an essential parameter for accurately determining the SOC, as it reflects the equilibrium potential across the battery's electrodes and inherently correlates with the battery's SOC. The precise characterisation of OCV as a function of SOC is critical for implementing effective SOC estimation strategies in energy management systems (EMSs). Firstly, based on the EC, a discrete state space equation with OCV as the state variable is constructed.

Assuming that the current direction is consistent with the arrow shown in Fig. 1, the EC dynamic electrical characteristics can be expressed as shown in (1).

$$\begin{cases} V_p = -\frac{1}{R_p C_p} V_p + \frac{1}{C_p} I \\ V_t = V_{oc} - V_p - IR \end{cases} \quad (1)$$

In (1), V_p is the terminal voltage of the RC network in EC, I is the battery current, V_t is the battery terminal voltage, V_{oc} is the battery OCV, R is the battery equivalent ohmic internal resistance, R_p and C_p are the current equivalent polarisation internal resistance and polarisation capacitance, respectively. Considering the nonlinear mapping relationship f_{ocv} between the OCV and the SOC of the battery, the derivative expression of V_{oc} is obtained as shown in (2).

$$V_{oc} = f_{ocv}(\text{SOC}) \cdot \frac{d\text{SOC}}{dt} = f'_{ocv}(\text{SOC}) \cdot \frac{I}{C_N} \quad (2)$$

Due to that, the total capacity C_N is usually much greater than the charging and discharging current I , research will consider V_{oc} as a slowly changing parameter and assume its derivative to be approximately 0. By comprehensively considering (1) and (2), a discretised state

space equation for lithium batteries with OCV as the state variable can be obtained, as shown in (3).

$$\begin{cases} x_{k+1} = Ax_k + Bu_k + w_k \\ y_k = Cx_k + Du_k + v_k \end{cases} \Leftrightarrow \begin{cases} \begin{bmatrix} V_{oc,k+1} \\ V_{p,k+1} \end{bmatrix} = \begin{bmatrix} 1 & 0 \\ 0 & \alpha \end{bmatrix} \begin{bmatrix} V_{oc,k} \\ V_{p,k} \end{bmatrix} + \begin{bmatrix} 0 \\ (1-\alpha)R_p \end{bmatrix} I_k + w_k \\ V_{t,k} = \begin{bmatrix} 1 & -1 \end{bmatrix} \begin{bmatrix} V_{oc,k} \\ V_{p,k} \end{bmatrix} - RI_k + v_k \end{cases} \quad (3)$$

In (3), x_k represents the state vector of the system time k , u_k represents the input of k , A and B represents the coefficient matrix of the state transition equation. $w_k \sim (0, Q_k)$ represents the model process noise that simulates the measurement error of the current sensor and the state equation at k , y_k represents the output of k , C and D represents the coefficient matrix of the measurement process. v_k represents the model measurement noise that simulates the measurement error of the voltage sensor and the output equation at the system time k . In the coefficient matrix A , $\alpha = e^{-\Delta t/R_p C_p}$, the sampling period Δt of the system is taken as 1s. R , R_p , and C_p are the unidentified model parameters. By using the Bayesian algorithm for online estimation of state variables V_{oc} and substituting them into the OCV–SOC relationship curve, SOC_V estimation based on the definition of OCV can be indirectly achieved.

The study conducts offline identification of the functional relationship between OCV and SOC and the parameters to be identified in the EC through low-current OCV–SOC mapping experiments and battery model parameter identification experiments. In the discrete state space equation, the ohmic internal resistance, polarisation internal resistance, and polarisation capacitance are the parameters to be identified, and they will change with changes in the battery state. The study not only considers the battery charge state but also considers the discharge rate impact of the battery on model parameters. The battery model parameter identification experiment is shown in Fig. 2.

The low-current OCV–SOC experiment utilised a direct relationship between the magnitude of the current and the degree of polarisation. By using a very small current, the difference between the diffusion rate of particles inside the battery and the electrochemical reaction rate is minimised as much as possible. Therefore, the terminal voltage during battery operation can be approximated as OCV, thus achieving online measurement of OCV during battery operation. The voltage prediction curve is generated by applying the identified parameters within an ECM, simulating the terminal voltage response under dynamic load conditions, based on SOC–OCV mapping and internal resistance changes. Then, the particles are filtered and updated based on their weights. Finally, the optimal estimation of the state is obtained through a posterior density function based on the updated particle swarm. In Bayesian filtering problems, state estimation can be simplified to solving the expected value

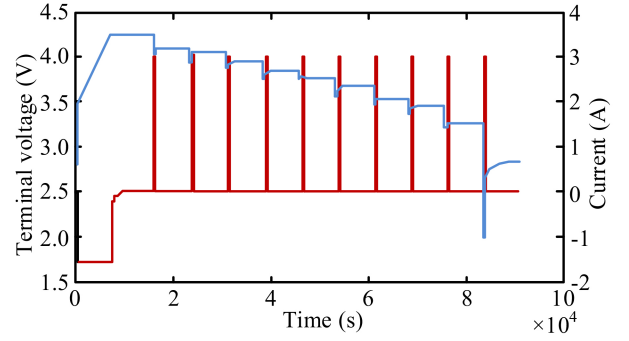


Figure 2. Battery model parameter identification experiment.

of a posterior distribution, as shown in (4).

$$E[g(x) | y_{1:T}] = \int g(x) p(x | y_{1:T}) dx \quad (4)$$

In (4), $g : \mathbb{R}^n \rightarrow \mathbb{R}^m$ is an arbitrary function and $p(x | y_{1:T})$ is the x posterior probability density under known measurement values y_1, \dots, y_T . In importance sampling $\pi(x | y_{1:T})$, based on obtaining samples using importance distribution, the expected value of the posterior distribution to be solved can be solved as shown in (5).

$$E[g(x) | y_{1:T}] = \int \left[g(x) \frac{p(x | y_{1:T})}{\pi(x | y_{1:T})} \right] \pi(x | y_{1:T}) dx \quad (5)$$

In (5), $x^{(i)}$ are the samples drawn from the importance distribution $p(x | y_{1:T})$ is the function whose expected value under the posterior distribution $x^{(i)} \sim \pi(x | y_{1:T})$, $i = 1, \dots, N$ we are interested in estimating, and N is the total number of samples. and based on this, MC approximation is performed on the importance sampling by integrating the expected integral and normalising the constant to obtain the expected value of the posterior distribution.

Assuming that the future operating conditions of the battery are known, the uncertainty introduced by battery state estimation is considered, specifically focussing on the standard deviation of the measurement error, denoted as σ . This standard deviation σ represents the measurement uncertainty in the current and voltage sensors, which affects the SOC estimation accuracy. The impact of different SOC definitions on the accuracy of the remaining discharge time (RDT) prediction is studied, with particular attention to how σ influences the SOC estimation and consequently the RDT forecast. The RDT is a predictive metric that estimates the duration for which a battery can continue to discharge until it reaches its predetermined lower voltage limit. The RDT is crucial for planning and managing energy consumption, particularly within a micro-grid energy storage system. Firstly, assuming the current moment is t , substituting the future current reference value \tilde{I} of the battery into the SOC definition equation can obtain the predicted SOC value as shown in (6).

$$SOC_{V,i} = SOC_{V,t} - \sum_t \frac{\tilde{I}_j \cdot \Delta t}{C_a}; j = t, t+1, \dots, i-1 \quad (6)$$

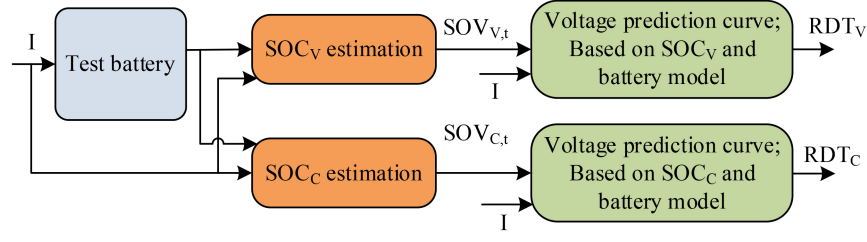


Figure 3. RDT prediction framework.

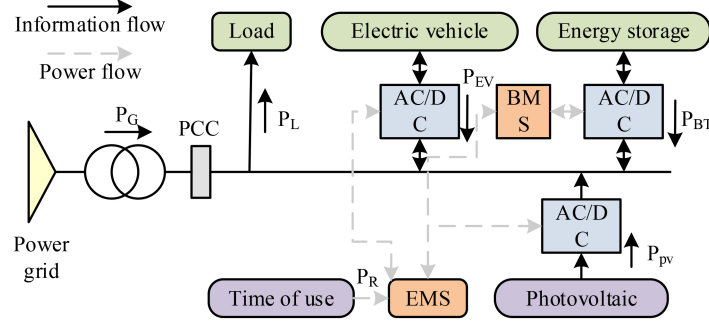


Figure 4. V2H system structure.

In (6), C_a is the discharge capacity of the battery, which has a certain nonlinear relationship with SOC_V . Based on the SOC_V estimation during a complete discharge process, the functional relationship is calculated as shown in (7).

$$C_a(SOC_{V,k+1}) = \frac{I_k}{SOC_{V,k} - SOC_{V,k+1}}; k = 1, 2, \dots, N \quad (7)$$

In (7), I_k represents the battery current at the moment k , $SOC_{V,k}$ and $SOC_{V,k+1}$ represent the estimated battery charge state at the moment, and N represents the total time length during a complete discharge process. The RDT prediction framework proposed in the study is shown in Fig. 3.

Then, based on the reference value of future operating conditions and the predicted value of SOC, combined with the measurement equation in the battery state space equation, the battery terminal voltage prediction curve is obtained. Then the predicted curve is compared with the lower voltage limit and the time when the battery discharge ends is found, which is the first time it falls below the lower voltage limit. Finally, the predicted RDT of the battery is obtained by calculating the difference between the end time of battery discharge and the current time.

3.2 Microgrid Energy Storage System Energy Management using Markov Chain Monte Carlo

The grid-connected microgrid studied consists of solar photovoltaic power generation systems, loads, energy storage batteries and battery management systems (BMSs), EVs, and EMS. These subsystems are connected to the AC bus of the microgrid through power electronic converters to

achieve energy exchange. The energy exchange between the microgrid and the power grid is carried out through PCC. Figure 4 shows the system's overall structure.

MCMC is a random sampling method that utilises the properties of Markov chains to obtain the stationary distribution of the desired parameters based on the state transition matrix. Then, using the idea of MC, repeatedly sampling the stationary distribution to obtain the estimated values of the parameters to be estimated. To construct an irreducible and non-periodic Markov chain with a stationary distribution consistent with the posterior distribution of the parameters to be solved, it is necessary to find a suitable state transition matrix. The detailed stationary conditions of Markov chains are used to determine whether the matrix P is a state transition matrix corresponding to a stationary distribution π . For non-periodic Markov chains, P and $\pi(x)$ satisfy (8) for all i and j .

$$\pi(i)P(i, j) = \pi(j)P(j, i) \quad (8)$$

The probability distribution $\pi(x)$ is said to be a stationary distribution of P . To achieve the parameters' optimal estimation to be solved, it is necessary to construct a state transition matrix P that satisfies detailed stationary conditions. The study adopts the MCMC sampling method and introduces an acceptance rate $a(i, j)$ to adjust the randomly given transition matrix Q , so that the entire process meets the detailed stationarity conditions. The calculation is shown in (9).

$$\pi(i)Q(i, j)a(i, j) = \pi(j)Q(j, i)a(j, i) \quad (9)$$

The range of $a(i, j)$ values is $[0, 1]$, indicating the probability that a randomly given matrix Q can serve as the target P . According to the detailed stationary conditions, the state transition matrix corresponding to

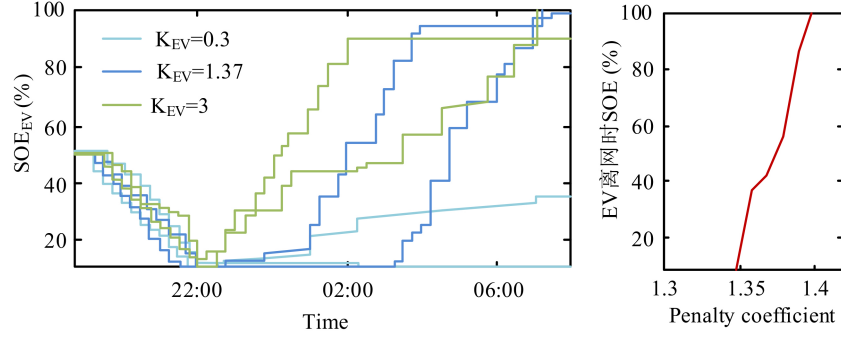


Figure 5. Penalty coefficient experiment.

parameters $\pi(x)$ to be solved can be expressed as $P(i, j) = Q(i, j)a(i, j)$. However, due to the small probability of the randomly selected matrix Q being close to the target matrix P , $a(i, j)$ in MCMC sampling is usually low, which affects the sampling efficiency. To solve this problem, the Metropolis–Hastings (M–H) algorithm was studied to improve it. The M–H algorithm is a widely used MCMC improvement algorithm that improves sampling efficiency by improving the calculation method of acceptance rate $a(i, j)$. $a(i, j)$ calculation is shown in (10).

$$a(i, j) = \min \left\{ \frac{\pi(j)Q(j, i)}{\pi(i)Q(i, j)}, l \right\} \quad (10)$$

When the prior distribution of the parameters to be solved is known, using M–H sampling can obtain a set of sampling points that converge to the parameter stationary distribution, that is, the posterior parameters distribution. By solving the mean of these sampling points, parameter inference based on maximum posterior estimation can be obtained.

To safely operate the household microgrid, avoid overcharging and discharging of the battery system, and extend battery service life, this study sets restrictions on the system as shown in (11).

$$\begin{cases} S_{BT, \min} \leq S_{BT, i} \leq S_{BT, \max} \\ P_{BT, \min} \leq P_{BT, i} \leq P_{BT, \max} \\ i = 1, 2, \dots, N \end{cases} \quad (11)$$

In (11), N is the total number of periods within the daily scheduling range, $S_{BT, i}$ is the battery energy state in the i time, $S_{BT, \min}$ and $S_{BT, \max}$ are the lower and upper limits of the energy state, respectively. The research settings are 20% and 100%. $P_{BT, i}$ is the battery power during the specified period. The maximum allowable charging power and maximum allowable discharge power of the energy storage battery system are $P_{BT, \min}$ and $P_{BT, \max}$, respectively, set at -6kW and 6kW in the research. The power integration method $S_{BT, i}$ is calculated as (12).

$$\begin{cases} S_{BT, i} = S_{BT, i-1} - \delta S_{BT, i-1} \\ \delta S_{BT, i-1} = P_{BT, i-1} \cdot T_S / E_{BT} \end{cases} \quad (12)$$

In (12), T_S is the duration of the period. $\delta S_{BT, i-1}$ indicates the amount of change in the battery energy state during the period from $i-1$ to i . E_{BT} is the total battery energy.

Considering the uncertainty brought by EVs in motion and the energy storage capacity of their batteries, when EVs are connected to the microgrid, they play a dual role in controllable load and mobile energy storage. EVs can be seen as a supplement and extension to energy storage batteries, thereby improving the microgrids' economic benefits. The study evaluates the impact of $K_{EV, i}$ value on $S_{EV, i}$ through experiments and designs a $K_{EV, i}$ regulatory strategy based on this. The experimental results are shown in Fig. 5.

From Fig. 5, as the $K_{EV, i}$ value of EV predicted off-grid time increases, the increase in EV energy state before the predicted off-grid time becomes more and more significant. The value of the penalty coefficient $K_{EV, i}$ has a significant impact on the SOE of EV in the i period. As the value of $K_{EV, i}$ increases, EVs tend to perform charging operations as controlled loads to meet their own electricity needs. On the contrary, EVs are more inclined to serve as mobile energy storage, discharging to supply power to the load during high electricity prices. A K_{EV} regulation strategy based on the probability of off-grid is studied and designed. When the off-grid probability of EV in the i period is less than 50%, the $K_{EV, i}$ value will be less than 1.35; on the contrary, the value of $K_{EV, i}$ will be greater than 1.4.

Assuming that the photovoltaic power generation, load power consumption, EV grid connection time, and initial SOE are known, the optimisation goal is to minimise the economic cost of one day. The costs considered include purchasing electricity cost from the power grid, EV battery discharge loss cost, and the economic penalty cost caused by insufficient EV energy. Ignoring additional costs such as operation and maintenance, the operating limitations of energy storage batteries and subsystems such as EVs are used as constraints, and the problem is constructed as (13).

$$\begin{aligned} & \min \sum_{i=1}^N [P_{G, i} \cdot P_{R, i} \cdot T_S + f_{EV, i} + f_{dis, i}] \\ & s.t. \\ & S_{BT, \min} \leq S_{BT, 0} + \sum_{k=0}^{i-1} \delta S_{BT, k} \leq S_{BT, \max} \end{aligned}$$

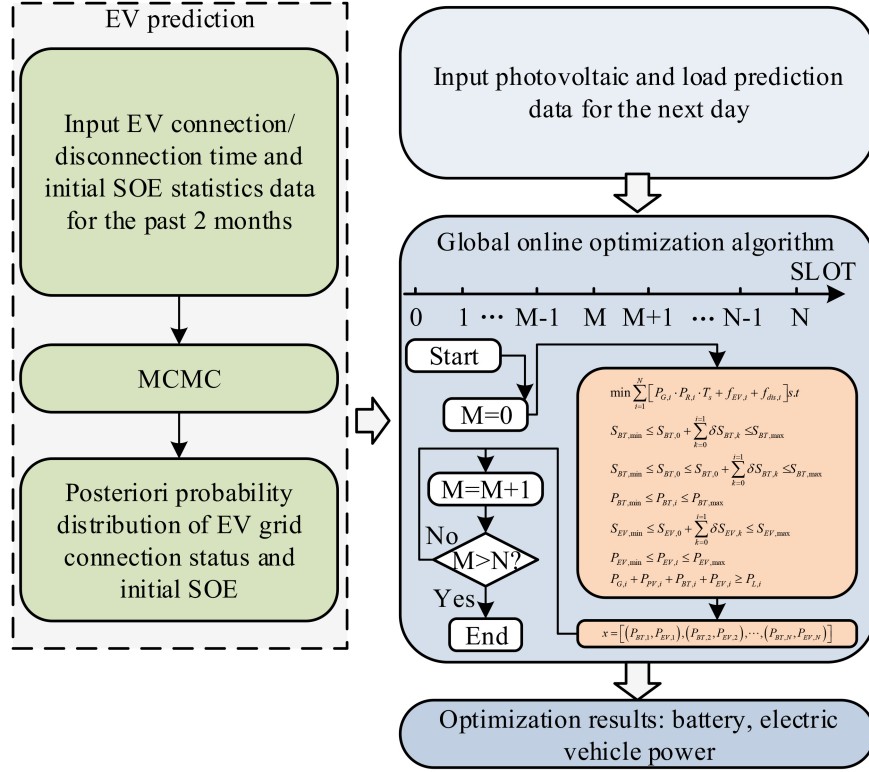


Figure 6. Microgrid energy management process.

$$\begin{aligned}
S_{BT,\min} &\leq S_{BT,0} \leq S_{BT,0} + \sum_{k=0}^{N-1} \delta S_{BT,k} \\
&\leq S_{BT,\max} \\
P_{BT,\min} &\leq P_{BT,i} \leq P_{BT,\max} \\
S_{EV,\min} &\leq S_{EV,0} + \sum_{k=0}^{i-1} \delta S_{EV,k} \leq S_{EV,\max} \\
P_{EV,\min} &\leq P_{EV,i} \leq P_{EV,\max} \\
P_{G,i} + P_{PV,i} + P_{BT,i} + P_{EV,i} &\geq P_{L,i} \quad (13)
\end{aligned}$$

The decision vector x to be optimised is shown in (14).

$$\begin{aligned}
x = [(P_{BT,1}, P_{EV,1}), (P_{BT,2}, P_{EV,2}), \\
\dots, (P_{BT,N}, P_{EV,N})] \quad (14)
\end{aligned}$$

In (14), $P_{G,i}$ is the grid power in the i period, $P_{R,i}$ is the grid electricity price in the i period, $P_{PV,i}$ is the photovoltaic power generation in i , and $P_{L,i}$ is the load electricity consumption in the i period. Microgrid energy management algorithms strategically dispatch and store energy, optimising economy and reliability through a multi-objective and constrained decision framework. The algorithm processes data from renewable energy sources such as solar and load demand in real time and integrates grid schedules with information on the status of EVs and battery storage. The goal is to operate microgrids at the lowest total cost, reducing the cost of purchasing electricity from the grid, battery life loss, and penalties for insufficient EVs. It solves complex optimisation problems, considers battery safety, and regulates EV loads, and achieves an efficient dynamic balance between supply and demand.

In the simulation experiment of the microgrid energy management algorithm, 3 kW photovoltaic equipment and daily electricity consumption statistics of residential users are used. The total energy capacity of energy storage batteries and EVs batteries is 8 kWh and 16 kWh, respectively. The specific energy management process of the microgrid is shown in Fig. 6.

In the state estimation and energy management of microgrid energy systems, particle filtering, and Markov chain MC methods are used for predicting the lifespan of ITO batteries. The study integrates key parameters, such as battery capacity, charge and discharge cycles, cycle efficiency, and temperature influence in detail for the characteristics and behaviour model of ITO batteries. These parameters are dynamically updated through particle filtering methods and applied to real-time estimation of SOH to predict the service life of batteries. Through this integration, EMS can more accurately predict battery life, and provide support for decision-making, such as maintenance scheduling and operational cost control, thereby improving the reliability and efficiency of the entire microgrid system.

4. State Estimation and Energy Management Simulation Experiment Analysis of Microgrid Energy Storage System

The study used low-current OCV-SOC mapping experiments to explore the nonlinear mapping relationship between the OCV and battery charge state. In terms of energy management in microgrid energy storage systems, research was conducted on 24-h dynamic economic

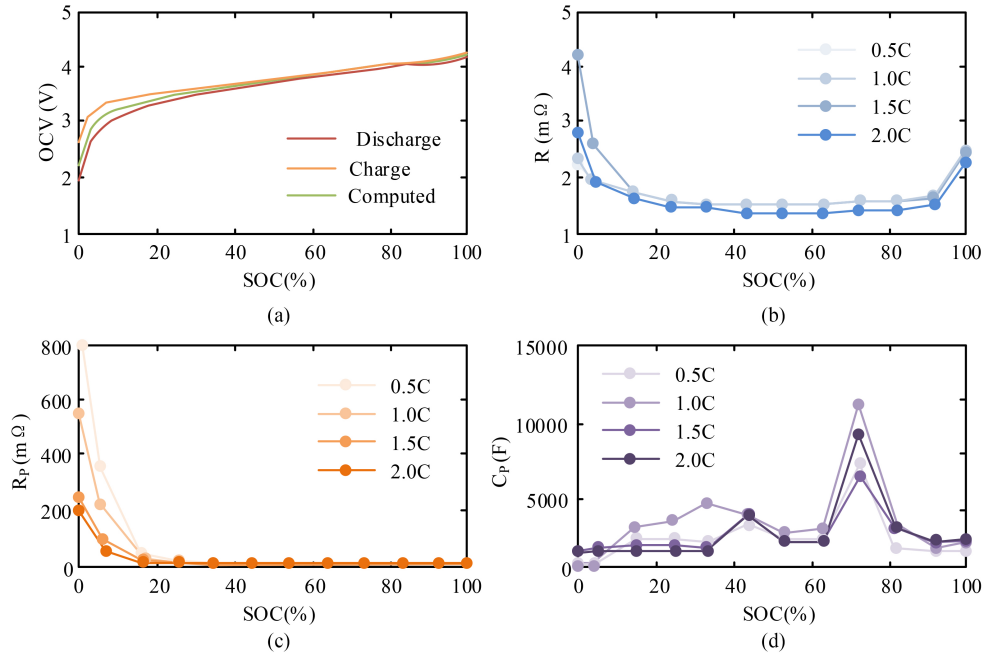


Figure 7. Offline identification results of battery model: (a) the nonlinear mapping relationship between OCV and SOC; (b) the nonlinear relationship between ohmic internal resistance and SOC; (c) nonlinear relationship between polarisation internal resistance and SOC; and (d) nonlinear relationship between polarisation capacitance and SOC.

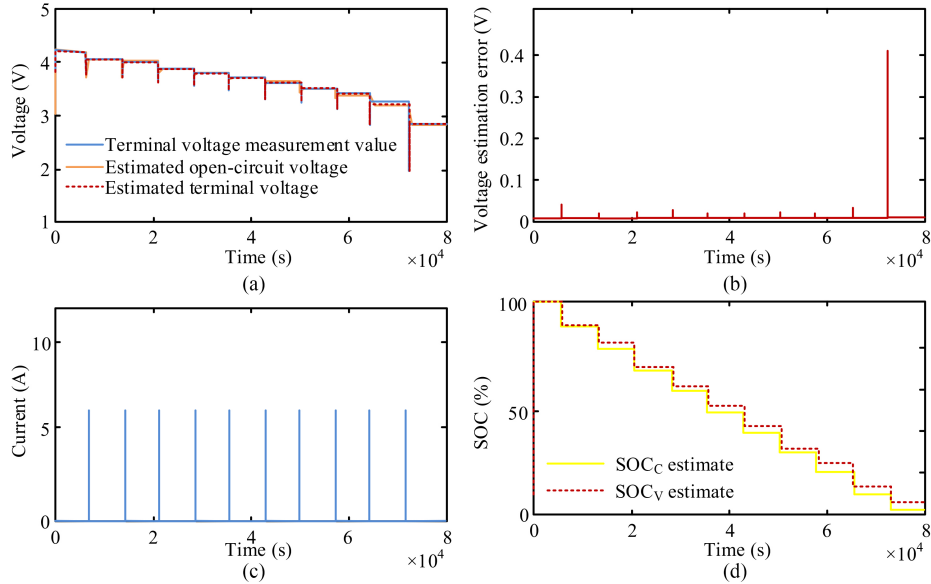


Figure 8. Estimation results of SOC under constant current operating conditions: (a) open circuit voltage estimation; (b) terminal voltage estimation; (c) battery current; and (d) comparison of estimated values.

scheduling experiments of microgrid energy storage systems in different scenarios. The experiment aimed to testify the operational effectiveness of the proposed energy management framework in the time-of-use electricity price scenario.

4.1 Charge Estimation and Life Prediction State Experimental Analysis for Lithium-ion Batteries

A low-current OCV–SOC mapping experiment was conducted to explore the mentioned nonlinear mapping

relationship. The battery experiment used the 18650 nickel cobalt manganese ternary lithium battery produced by Sony, with the model being VCT6. The parameters of the test battery are shown below [23].

The experimental platform used for battery experiments mainly consists of three parts. The battery testing system produced by Xinwei Company, model CT-8004-5V200A-NTFA, has the function of serving as a power source and controllable load for testing batteries. It can perform various battery experiments such as constant current and constant capacity testing, pulse charging and discharging testing, *etc.* The upper computer was

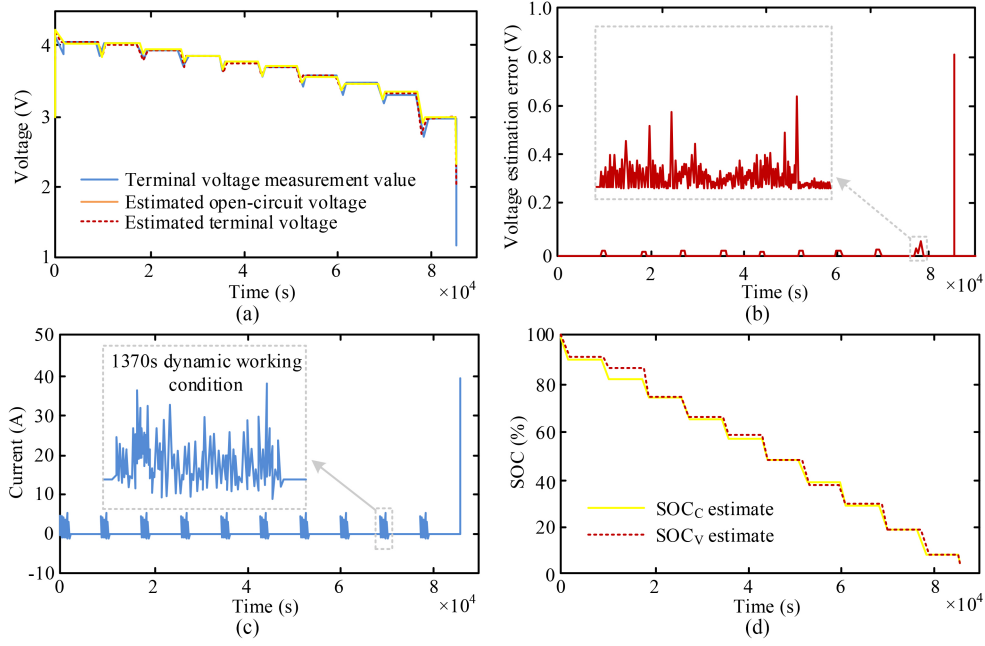


Figure 9. SOC estimation results under dynamic operating conditions: (a) open circuit voltage estimation; (b) terminal voltage estimation; (c) battery current; and (d) comparison of estimated values.

Table 1
The Experimental Battery Parameters

Parameter	Value
Rated capacity	3000 mAh
Lower limit voltage	2.0 V
Upper limit voltage	4.25 V
Lower limit temperature	-20 °C
Upper limit temperature	60 °C

used to set the operation process of the battery testing system and display experimental data in the form of a graphical interface. The thermostat provided stable ambient temperature conditions for testing the tested battery. In addition, to evaluate the computational efficiency of the proposed algorithm, the CPU time required during the operation of the power estimation and life prediction algorithms was recorded. The calculation specification used the relevant algorithm to describe the state of the battery, which was implemented in the standard data processing flow. The algorithm was executed on a computer equipped with an Intel Core i7-9700 CPU @ 3.00GHz processor with 16GB of RAM. In the experimental analysis of the battery state, the average CPU time required was 45 s, of which the pretreatment of the experimental data took 10 s, and the actual running time of the mapping algorithm was 35 s, which showed the feasibility of the processing algorithm in terms of computational efficiency. All tests were conducted in a Windows 10 operating system environment without external graphics processing unit (GPU) acceleration,

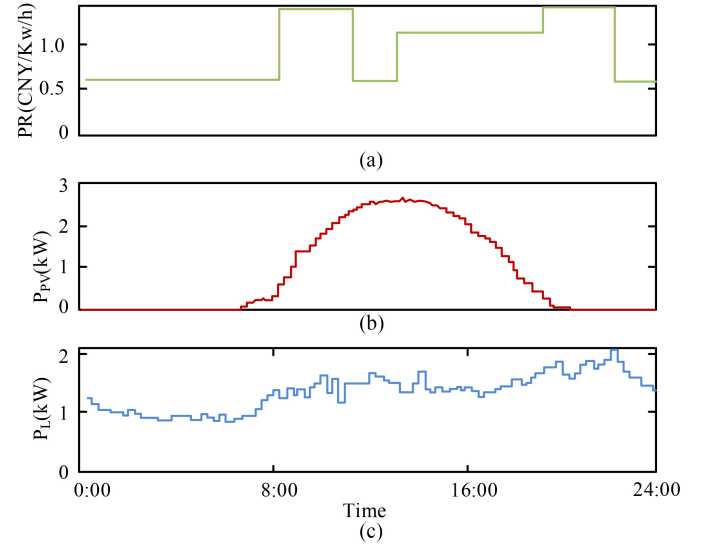


Figure 10. Prediction curve: (a) time of use; (b) photovoltaic power generation prediction; and (c) load electricity consumption prediction.

using MATLAB R2020a as the development and execution environment.

At the same time, the study also conducted battery model parameter identification experiments to obtain the nonlinear relationship between ohmic internal resistance, polarisation internal resistance, and polarisation capacitance with battery SOC under different current conditions. The results of two sets of experiments are shown in Fig. 7.

In Fig. 7(a), the OCV shows an approximately linear change in the SOC range of 20%–100%, while it shows an accelerated decrease trend when the SOC ranges from 10% to 0%. In Fig. 7(b), the variation trend of ohmic

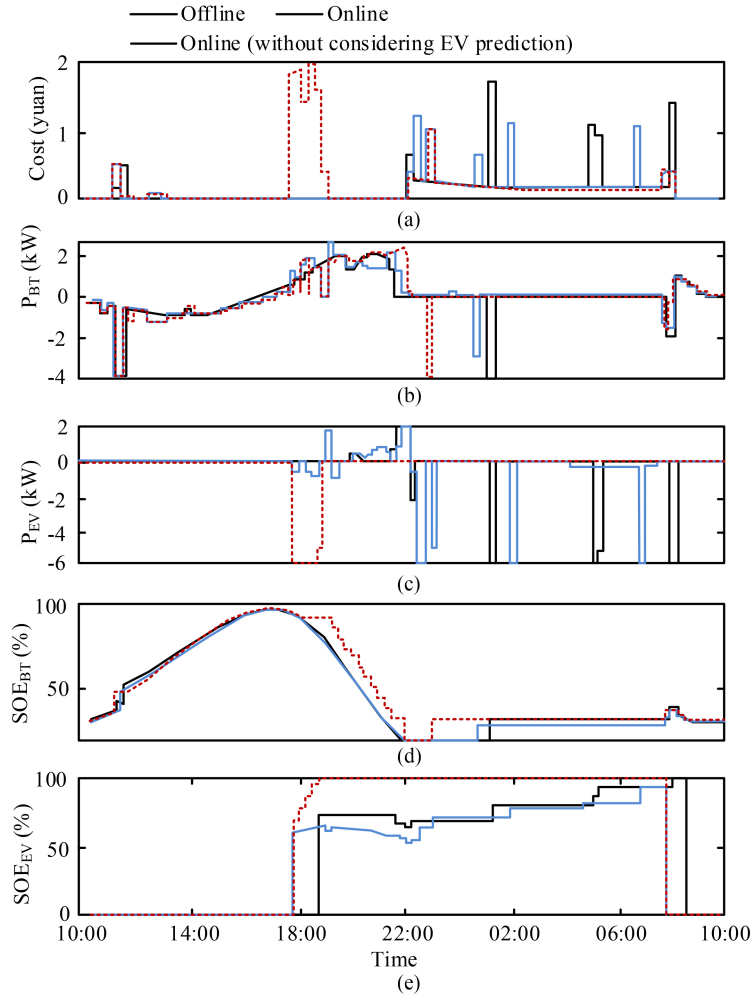


Figure 11. Simulation results of three EMS strategies in EV conventional travel under the time of use electricity price scenario: (a) cost simulation results; (b) P_{BT} simulation results; (c) P_{EV} simulation results; (d) SOE_{BT} simulation results; and (e) SOE_{EV} simulation results.

internal resistance is the same under different current conditions, decreasing first and then increasing with the discharge process, and there is a longer plateau period in the middle range of SOC. In Fig. 7(c) and (d), polarisation internal resistance and capacitance maintain a similar trend with changes in SOC. Results indicated that the current has a small impact on the model parameters, and the relationship curve accuracy between the model parameters and SOC has a significant impact on the model accuracy.

The algorithm's SOC estimation results were compared and analysed under 2.5C constant current and dynamic operating conditions to verify the method's effectiveness. The estimated results of SOC under constant current operating conditions are shown in Fig. 8.

In Fig. 8(a) and (b), when there is a significant change in battery current, there may be some error in the estimated value. However, as the current stabilised, the error gradually decreased, indicating that the algorithm can effectively track the measured value. During the battery soak process, the estimated open-circuit voltage gradually approached the measured value, accurately achieving an online estimation of open-circuit voltage. Figure 8(c)

shows the battery current during the experiment, where the purpose of the quiescent operation is to evaluate the estimation effect of the OCV. Figure 8(d) compares the results of two types of SOC estimation. During the constant current discharge process, both show a downward trend. During the quiescent process, the estimation results based on the definition of OCV had a positive steady-state error compared to the results based on the definition of ampere-hour integration. Considering that the polarisation effect during battery discharge may affect SOC, the estimation algorithm based on the definition of OCV can more accurately reflect the battery's actual behavioural characteristics, considering the impact of the polarisation effect on SOC. Its estimation results under dynamic operating conditions are shown below.

In Fig. 9(a) and (b), the estimated terminal voltage almost coincides with the measured value, and during the battery soak process, the estimated open-circuit voltage tends to approach the measured value, indicating that the algorithm can achieve good open-circuit voltage estimation and terminal voltage tracking capabilities under dynamic conditions. In Fig. 9(d), SOC estimation results based on

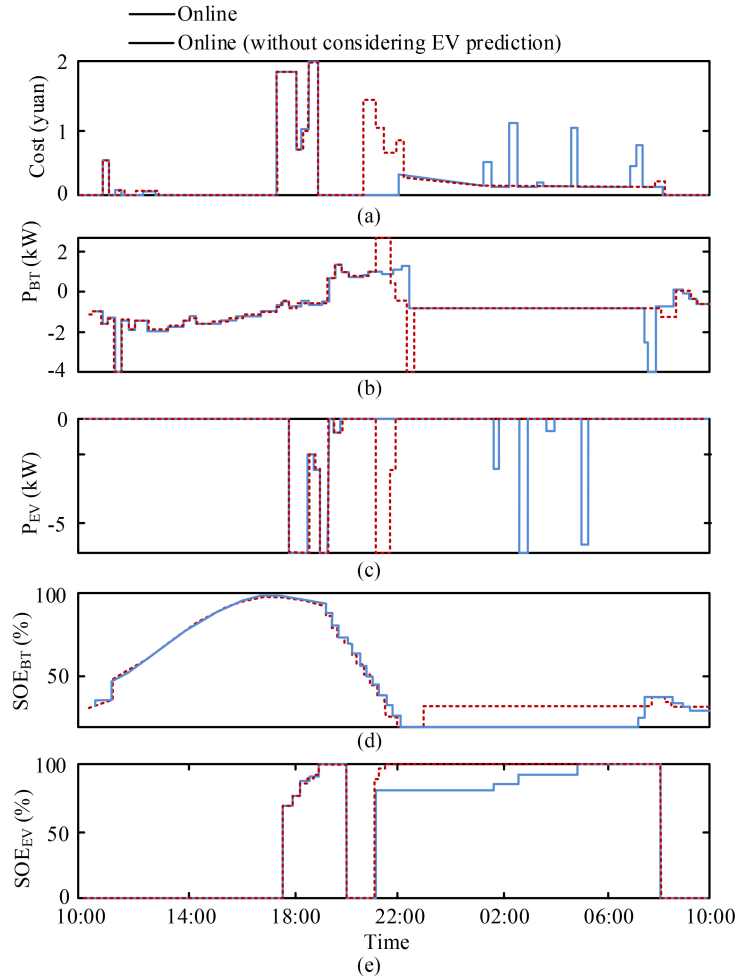


Figure 12. Simulation results of EV unconventional travel under time-of-use electricity price: (a) cost simulation results; (b) P_{BT} simulation results; (c) P_{EV} simulation results; (d) SOE_{BT} simulation results; and (e) SOE_{EV} simulation results.

the definition of OCV have a positive steady-state error. This indicates that the proposed estimation algorithm based on the definition of OCV can better reflect the recovery effect caused by the polarisation effect under dynamic operating conditions.

4.2 Energy Management of Microgrid Energy Storage System Simulation Experiment

The study analysed the 24-h dynamic economic dispatch results of microgrid energy storage systems in different scenarios. The experiment aimed to test the operational effectiveness of the energy management framework in the time-of-use electricity price scenario. The predicted curves of time-of-use electricity price, photovoltaic power generation, and load power consumption are shown in Fig. 10. To determine the predicted curves for time-of-use electricity price, photovoltaic power generation, and load power consumption, the study employed machine learning algorithms that utilised historical data as input variables. For the prediction of time-of-use electricity price, market historical data along with demand and supply patterns were analysed. The photovoltaic power generation prediction model considered historical light intensity data and temporal variables to project the generation curve.

Load power consumption forecasted leverage residential electricity usage statistics to identify daily consumption peaks. These predictive models were crucial for the development of an effective energy management framework within the microgrid.

In Fig. 10, the prediction curve is the output of historical data and machine learning techniques. In the prediction of photovoltaic power generation, the model used the historical data of light intensity and time as input to reveal the trend of daily power generation over time, in which the red curve shows that the power generation reaches the highest point at noon and decreases significantly at both ends of the morning and evening. Load electricity consumption forecast adopted the historical statistical data of residential electricity consumption as input and obtained the peak period of daily electricity consumption through analysis, which was represented by two significant peaks of the blue curve in the morning and evening. According to this, it is found that at noon, the photovoltaic power generation reached a peak of about 2 kW, while at 8 AM and 6 PM, the value was close to zero. Daily residential electricity consumption forecasts showed that the load increased rapidly to about 1 kW in the morning and may rise to a higher level of about 1.5 kW in the evening. These data reflected that there may be a

mismatch between residential peak electricity consumption and photovoltaic power supply, indicating the necessity of adjusting the energy storage system strategy. To keep the EV connected to the grid within a scheduling cycle (24 h), the scheduling start time was set to 10:00 AM. The simulation results of three EMS strategies under the time of use electricity price during EV conventional travel are shown in Fig. 11.

In Fig. 11(a), at around 18:00, the results of the optimisation framework without considering EV prediction have additional costs compared to the optimisation framework proposed in the study. This is because the optimisation framework did not know the probability of EV leaving the grid. To meet the power demand of EVs leaving the grid, the penalty coefficient needed to be maintained at a large value to enable EV to charge as soon as possible and maintain SOC at a certain level after connecting to the microgrid. The changes in EV power and SOC under this optimisation framework are shown in Fig. 11(c) and (e). The optimisation framework that did not consider EV prediction only charged EV as a controllable load, reducing its ability to increase economic benefits for microgrids as mobile energy storage. Figure 12 shows the simulation results of EV unconventional travel under time-of-use electricity price.

Figure 12 shows the comparison results between the proposed optimisation framework and the optimisation framework without considering EV prediction in the case of unconventional EV travel (19:45–20:45). According to the adjustment strategy of the penalty coefficient, after the EV first arrived at the microgrid according to the regular travel pattern (at 17:30), it needed to send the next unconventional travel plan to the EMS. The EMS adjusted the penalty coefficient based on this to meet the electricity demand of the EV’s unconventional travel. Therefore, both optimisation frameworks optimised the EV after its initial connection to the microgrid. However, when the EV was connected to the microgrid for the second time (at 20:45), the optimisation framework without considering EV prediction cannot determine the predicted time of the next departure of the EV from the microgrid. Therefore, it was necessary to immediately charge to meet the electricity demand when the EV left the grid at unknown times in the future, resulting in an increase in system operation costs.

5. Conclusion

A particle filter-based method is proposed for estimating the SOC and predicting the lifespan of ITO batteries, crucial for addressing energy management challenges in microgrid energy storage systems. Additionally, the integration of Markov chain MC techniques enhances energy management within these systems. The findings indicate that the SOC estimates, derived from the definition of OCV, exhibit high accuracy. Notably, a nearly linear relationship between OCV and SOC was observed within the 20%–100% SOC range. Simulations of energy management in a microgrid storage system, incorporating 3 kW photovoltaic modules and daily residential energy usage statistics, were conducted. The

Symbol Table

Symbol	Definition
OCV	Open Circuit Voltage
SOC	State of Charge
Rd	Resistor simulating self-discharge and battery capacity characteristics
CN	Current controlled current source
R	Battery equivalent Ohmic internal resistance
Rp	Polarisation internal resistance
Cp	Polarisation capacitance
Vp	Terminal voltage of the RC network
Vt	Battery terminal voltage
I	Battery current
focv	Nonlinear mapping relationship between OCV and SOC
dSOC/dt	Rate of change of SOC with time
xk	State vector of the system at time k
uk	Input of the system at time k
A, B	Coefficient matrices of the state transition equation
wk	Model process noise at time k
yk	Output of the system at time k
C, D	Coefficient matrices of the measurement process
vk	Model measurement noise at time k
Δt	Sampling period of the system
SOCV	SOC estimation based on the definition of open circuit voltage
Qk	Covariance of the process noise wk

simulations revealed that the energy storage battery and the EVs battery had capacities of 8 kWh and 16 kWh, respectively. The implementation of a time-of-use electricity pricing model demonstrated that the optimisation framework, which included EV usage predictions, yielded lower operational costs than frameworks without such predictions, thereby enhancing the economic efficiency of energy management. These results substantiate that the methodologies employed facilitate precise SOC estimation and battery lifespan prediction, alongside improved energy management for storage systems.

References

- [1] Y. Li, R. Wang, and Z. Yang, Optimal scheduling of isolated microgrids using automated reinforcement learning-based multi-period forecasting, *IEEE Transactions on Sustainable Energy*, 13(1), 2021, 159–169.

- [2] R. Carli, G. Cavone, T. Pippia, B. De Schutter, and M. Dotoli, Robust optimal control for demand side management of multi-carrier microgrids, *IEEE Transactions on Automation Science and Engineering*, 19(3), 2022, 1338–1351.
- [3] L. Yin, K.N. Kim, A. Trifonov, T. Podhajny, and J. Wang, Designing wearable microgrids: Towards autonomous sustainable on-body energy management, *Energy & Environmental Science*, 15(1), 2022, 82101.
- [4] N. Ju, J. Awan, R. Gong, and V. Rao, Data augmentation MCMC for Bayesian inference from privatized data, *Proc. Advances in Neural Information Processing Systems*, 2022, 12732–12743.
- [5] Q. Qin, and J.P. Hobert, Wasserstein-based methods for convergence complexity analysis of MCMC with applications, *The Annals of Applied Probability*, 32(1), 2022, 124–166.
- [6] Y. Fang, B. Luo, T. Zhao, D. He, B. Jiang, and Q. Liu, ST-SIGMA: Spatio-temporal semantics and interaction graph aggregation for multi-agent perception and trajectory forecasting, *CAAI Transactions on Intelligence Technology*, 7(4), 2022, 744–757.
- [7] B. Duan, Q. Zhang, F. Geng, and C Zhang, Remaining useful life prediction of lithium-ion battery based on extended Kalman particle filter, *International Journal of Energy Research*, 44(3), 2020, 1724–1734.
- [8] V. Malviya and R. Kala, Trajectory prediction and tracking using a multi-behaviour social particle filter, *Applied Intelligence*, 52(7), 2022, 7158–7200.
- [9] P. Kamsing, P. Torteeka, and S. Yooyen, An enhanced learning algorithm with a particle filter-based gradient descent optimizer method, *Neural Computing and Applications*, 32, 2020, 12789–12800.
- [10] T. Meng, Z. Lin, and Y.A. Shamash, Distributed cooperative control of battery energy storage systems in DC microgrids, *IEEE/CAA Journal of Automatica Sinica*, 8(3), 2021, 606–616.
- [11] A. Khalid, A. Stevenson, and A.I. Sarwat, Overview of technical specifications for grid-connected microgrid battery energy storage systems, *IEEE Access*, 9, 2021, 163554–163593.
- [12] A. Joshi, A. Suresh, and S. Kamalasan, Grid frequency regulation based on point of common coupling angle deviation control of distributed energy resources with fully active hybrid energy storage system, *IEEE Transactions on Industry Applications*, 57(5), 2021, 4473–4485.
- [13] M. Daneshvar, B. Mohammadi-Ivatloo, K. Zare, and S. Asadi, Transactive energy management for optimal scheduling of interconnected microgrids with hydrogen energy storage, *International Journal of Hydrogen Energy*, 46(30), 2021, 16267–16278.
- [14] M.M. Islam, M. Nagrial, J. Rizk, and A Hellany, Dual stage microgrid energy resource optimization strategy considering renewable and battery storage systems, *International Journal of Energy Research*, 45(15), 2021, 21340–21364.
- [15] C. Pozna, R.E. Precup, E. Horváth, and E.M. Petriu, Hybrid particle filter–particle swarm optimization algorithm and application to fuzzy controlled servo systems, *IEEE Transactions on Fuzzy Systems*, 30(10), 2022, 4286–4297.
- [16] A. Gunatilake, S. Kodagoda, and K. Thiyagarajan, A novel UHF-RFID dual antenna signals combined with Gaussian process and particle filter for in-pipe robot localization, *IEEE Robotics and Automation Letters*, 7(3), 2022, 6005–6011.
- [17] M. Ballezio, A. Jasra, E. von Schwerin, and R. Tempone, A Wasserstein coupled particle filter for multilevel estimation, *Stochastic Analysis and Applications*, 41(5), 2023, 820–859.
- [18] T. Dalgaty, N. Castellani, C. Turck, K.E. Harabi, D. Querlioz, and E. Vianello, In situ learning using intrinsic memristor variability via Markov chain Monte Carlo sampling, *Nature Electronics*, 4(2), 2021, 151–161.
- [19] E. Srilakshmi and S.P. Singh, Energy regulation of EV using MILP for optimal operation of incentive based prosumer microgrid with uncertainty modelling, *International Journal of Electrical Power & Energy Systems*, 134(1), 2022, 1–12.
- [20] H. Bakhtiari, J. Zhong, and M. Alvarez, Predicting the stochastic behavior of uncertainty sources in planning a stand-alone renewable energy-based microgrid using Metropolis-coupled Markov chain Monte Carlo simulation, *Applied Energy*, 290(5), 2021, 1–15.
- [21] O.M. Salim, A. Aboraya, and S.I. Arafa, New cascaded controller for a standalone microgrid-connected inverter based on triple action controller and particle swarm optimization, *Institution Engineering Technology Generation Transmission & Distribution*, 14(17), 2020, 3389–399.
- [22] D.A. Gadanayak and R.K. Mallick, Microgrid protection using iterative filtering, *International Transactions on Electrical Energy Systems*, 30(3), 2020, 1–22.
- [23] C.D. Quilty, D. Wu, W. Li, D.C. Bock, L. Wang, L.M. Housel, A. Abraham, K.J. Takeuchi, A.C. Marschilok, and E.S. Takeuchi, Electron and ion transport in lithium and lithium ion battery negative and positive composite electrodes, *Chemical Reviews*, 123(4), 2023, 1327–1363.

Biographies



Libin Yang was born in July 1985, in Guangrao, Shandong Province, China. He received the Doctoral degree in power system and automation from Shenyang University of Technology in 2022. His research focuses on new energy and energy storage grid connection technology. Since March 2023, he has been the Director of the New Energy Grid Connection Technology Laboratory, Economic and Technological Research Institute (Clean Energy Development Research Institute) of State Grid Qinghai Electric Power Company.



Tingxiang Liu was born in September 1992, in Xinyang, Henan, China. He received the master's degree in electrical engineering from Lanzhou University of Technology in 2019. His research focuses on new energy and energy storage grid connected power generation technology. Since 2019, he has been in charge of the New Energy Grid Connection Technology Laboratory, Economic and Technological Research Institute (Clean Energy Development Research Institute) of State Grid Qinghai Electric Power Company.



Zhengxi Li was born in October 1990, in Haidong, Qinghai Province, China. He is currently pursuing an in-service Doctoral degree in electrical engineering with the North China Electric Power University. His research focuses on new energy and energy storage grid connected power generation technology. Since August 2023, he has been working as a Specialist with the Economic and

Technological Research Institute (Clean Energy Development Research Institute) of State Grid Qinghai Electric Power Company and the Deputy Director of the New Energy Industry Development Research Center.



Na An was born in October 1997, in Xining, Qinghai, China. She received the bachelor's degree in electrical engineering and automation from Qinghai University in 2020. Since 2020, she has been responsible for the Economic and Technological Research Institute (Clean Energy Development Research Institute) of State Grid Qinghai Electric Power Company.



Wanpeng Zhou was born in October 1994, from Xining City, Qinghai Province, China. He received the master's degree in electrical engineering from Qingdao University in 2020. His research focuses on new energy and energy storage power generation grid connection technology. Since 2020, he has been responsible for actively supporting new energy technology at the Economic and Technological Research

Institute, State Grid Qinghai Electric Power Company (State Grid Qinghai Electric Power Company Clean Energy Development Research Institute).